Available online at www.sciencedirect.com
ScienceDirect
Polymer 48 (2007) 2007–2013
polymer
www.elsevier.com/locate/polymer

Interfacial polymerization of pyrrole and in situ synthesis of polypyrrole/silver nanocomposites

Panagiotis Dallas [a], Dimitrios Niarchos [a], Daniel Vrbanic [b], Nicholaos Boukos [a], Stane Pejovnik [b], Christos Trapalis [a], Dimitrios Petridis [a,*]

[a] NCSR Demokritos, Institute of Materials Science, Patriarhou Grigoriou & Neapoleos, Athens 15310, Greece
[b] Department of Inorganic Technology and Materials, Faculty of Chemistry and Chemical Technology, University of Ljubljana, Askerceva 5, 1000 Ljubljana, Slovenia

Received 17 November 2006; received in revised form 15 January 2007; accepted 20 January 2007
Available online 31 January 2007

Abstract

We present a new synthetic approach leading to the formation of polypyrrole architectures in submicron level and to silver/polypyrrole nanocomposites via an interfacial polymerization in a water/chloroform interface. The oxidizing agent was either Ag(I) or Fe(III). In the first case, silver nanoparticles resulted. The mean diameter of the polypyrrole structures is in the range of 200–300 nm according to the addition or not of various surfactants. The progress of the reaction was studied by UV–visible spectroscopy, which also revealed the formation of a polaron band during the growth of the oligomers. The crystal structure of the polymers was examined by X ray diffractometry and all samples appeared to be amorphous, while the samples were further characterized by thermogravimetric analysis and FT-IR spectroscopy.

Keywords: Silver nanocomposites; Interfacial polymerization; Polypyrrole

1. Introduction

Recent advances in the field of electrically conducting polymers have attracted an increasing interest in the study of submicron or nanostructural electroactive polymers [1]. For example, polyaniline nanotubes or nanofibers with diameters less than 100 nm have been synthesized by polymerizing the monomer in either ''hard'' or ''soft'' templates. The former includes zeolites [2], polycarbonate [3], anodized alumina [4], micelles [5], liquid crystals [6] and polyacids [7]. Recently, the synthesis of polyaniline [8] and polypyrrole nanotubes [9] or nanofibers via a template seeding route has been described. The size of these polymeric nanotubes can be controlled in the range of 20–100 nm according to the kind of template used in the synthesis [9]. Expanding the reported structures that fall within the submicron level, hollow polyaniline or polypyrrole spheres have also been reported [10]. Moreover, interfacial polymerization has been applied for the synthesis of polyaniline nanofibers [11]. However, several factors affecting the formation of the various nanostructures and the corresponding polymerization mechanisms are yet to be clearly identified.

In addition, silver nanoparticles exhibit significantly interesting conductive and optical properties [12]. Their size and shape dependent optical properties arise from their surface plasmon resonance frequency, characteristic of noble metals with free electrons such as Au and Ag which results in a characteristic absorption in the UV–visible spectrum [13]. The novel features of metal nanoparticles and conductive polymers lead to an increasing interest in the synthesis of composite materials consisting from finely and homogenously dispersed nanoparticles in polymer matrices [14]. Specifically Ag(I) has been previously reported to initiate the polymerization of pyrrole leading to polypyrrole and silver nanostructures

* Corresponding author. Tel.: +30 2106503343; fax: +30 2106519430.
E-mail address: dpetrid@ims.demokritos.gr (D. Petridis).

0032-3861/$ - see front matter © 2007 Elsevier Ltd. All rights reserved.
doi:10.1016/j.polymer.2007.01.058

[14a]. However, one major problem when synthesizing nanocomposite materials derived from the dispersion of nanoparticles in polymer matrices is the aggregation of nanoparticles [15].

This article describes the polymerization of pyrrole in the boundary of two immiscible solvents which can be applied for the synthesis of silver/polypyrrole nanocomposites. To our knowledge no previous work has been reported to describe the interfacial polymerization of pyrrole. An important aspect of the interfacial polymerization procedure is that it enables the addition of various surfactant molecules, either negatively or positively charged, to the organic phase or even hydrophilic surfactants to the aqueous phase. As a result, the morphological and structural characteristics of the polymer can be easily controlled according to the reaction conditions. The aim of our work is to extensively study the interfacial polymerization of pyrrole and to synthesize nanocomposite materials with finely dispersed silver nanoparticles of low mean diameter.

2. Experimental part

2.1. Chemicals

Reagent grade $Fe(NO_3)\cdot 9H_2O$, dodecyltrimethylammonium bromide (DTAB) and sodium dodecylsulfate (SDS) were used as received from Aldrich, Eastman and Fluka, respectively. Pyrrole (Aldrich) was distilled under nitrogen before use. $Ag(NO_3)$ was purchased from Riedel De Haan (99.5%).

2.2. Synthesis of polypyrrole

The synthetic procedure involves polymerization of pyrrole in a water/chloroform interface with pyrrole monomer and surfactants added to the organic phase, while $Fe(NO_3)\cdot 9H_2O$ to the aqueous phase. The aqueous solution was slowly added to the organic medium. In a typical preparation, a solution of 300 mg $Fe(NO_3)\cdot 9H_2O$ (0.75 mmol) in 15 ml of H_2O was slowly spread to 15 ml chloroform containing 0.8 ml of pyrrole monomer (11 mmol) and 0.7 mmol of DTAB or SDS. As the reaction proceeded, without stirring, a black film appeared at the interface. A 24 h reaction time was sufficient to complete the growth of the polypyrrole film. The byproducts of the reaction were easily removed due to their solubility in the aqueous or organic media. The insoluble in organic or polar solvents film was isolated by decanting the solvents, washed several times with water and alcohol and air dried. During the reaction progress pyrrole oligomers were detected in the aqueous phase. Their solubility allowed the recording of the UV–visible spectra. The polypyrrole obtained without surfactants is designated as PPy/NO_3, while the samples with SDS and DTAB as PPy/SDS and PPy/DTAB, respectively.

2.3. Synthesis of silver/polypyrrole nanocomposites

$AgNO_3$ (130 mg, 0.75 mmol) used as an oxidant was dissolved in 15 ml H_2O and the solution was added to 7 mmol of pyrrole (0.5 ml) in 15 ml of chloroform. The polymerization proceeded as described when Fe(III) was used as an oxidant. Sample name: PPy/Ag.

3. Characterization techniques

X ray diffraction patterns were recorded on powder samples by a Siemens 500 Diffractometer. Cu Kα radiation ($\lambda = 1.5418$ Å) was used with a scan rate 0.03°/2 s. Thermogravimetric measurements (TGA) were recorded on a Perkin–Elmer Pyris TGA/DTA apparatus under a continuous air flow with a heating rate 10 °C/min. For the thermal analysis measurements about 3–4 mg of each sample was used. Infrared (FT-IR) spectroscopy studies were performed on a Bruker Equinox 55/S model spectrometer. The specimen was made by mixing the corresponding composites with KBr (Aldrich, 99%, FT-IR grade). The samples were dried at 60 °C for 24 h before all measurements. UV–visible spectra of the aqueous solution were collected on a Shimadzu 2100 spectrometer in quartz cuvettes. Scanning electron microscopy images were recorded on a Carl Zeiss Supra 35 VP. Transmission electron microscopy images were recorded on a Philips CM20 operated at 200 kV.

4. Results and discussion

For the synthesis of polypyrrole films ferric ions ($Fe(NO_3)\cdot 9H_2O$) or silver cations ($Ag(NO_3)$) were used as oxidizing agents. Following the transfer of reagent solutions to the reaction vessel the polymerization started and after a few hours a polypyrrole film was formed at the interface. It is important to note that while the oxidative polymerization of pyrrole in solution is a rapid and not controllable reaction, the corresponding reaction at the interface of two immiscible liquids involves the diffusion of the reactants to the interface, and thus the growth of the film is slow and completed in almost 24 h. We also note that while in the case of interfacial polymerization of aniline, the oxidized and protonated polyaniline are soluble in water and migrate to the aqueous phase, in the pyrrole case the resulting polypyrrole is insoluble in common organic or polar solvents and thus after completion of reaction, a black film is observed at the interface that is easily separated and dried.

The growth of the interfacial polypyrrole film can be inferred by tracking the evolution of the oligomers in the aqueous phase. Although, the oxidative polymerization occurs mainly at the interface, a small percentage of the pyrrole monomers diffuses to the aqueous phase where limited bulk polymerization leads to the formation of soluble pyrrole oligomers. When the molecular weight of the oligomers increases the polymers become insoluble in both solvents. It is interesting to note that in the absence of surfactant, the aqueous phase acquires a light red color within a few minutes, in contrast to a light green when SDS and DTAB were added.

The UV–visible spectra of the oligomers formed in the aqueous phase are shown in Fig. 1. At the start of reaction the spectrum is that of $Fe(H_2O)_6^{3+}$. As the reaction proceeds

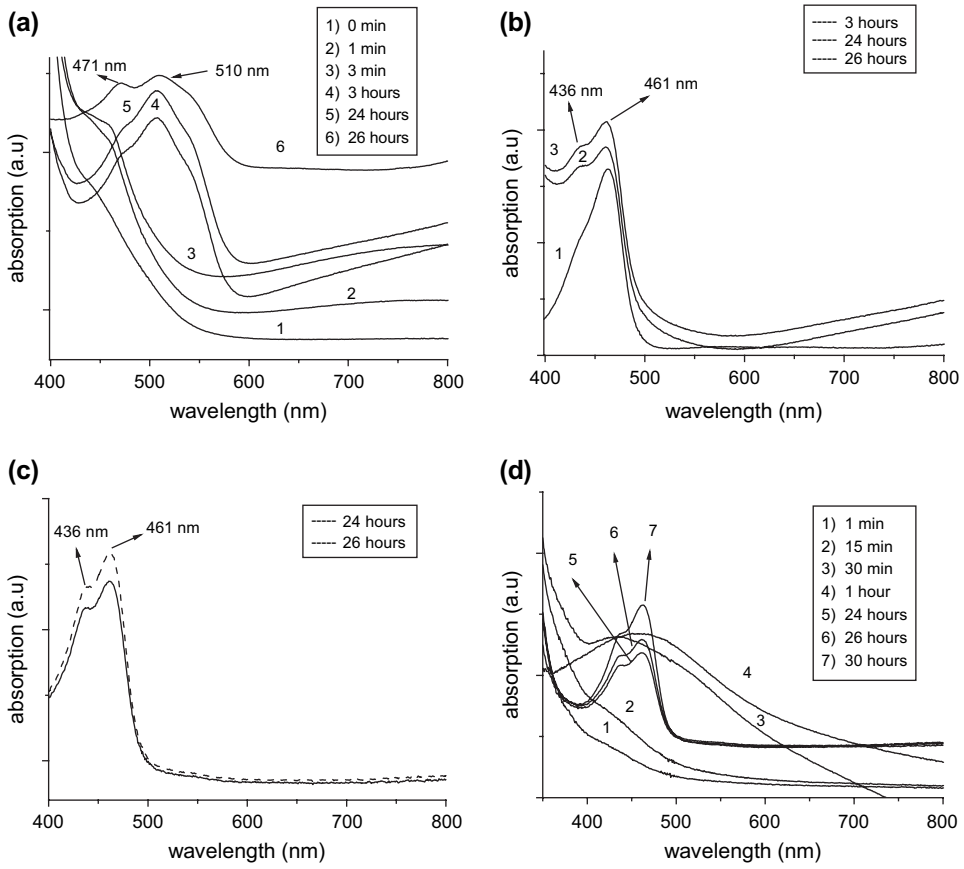

Fig. 1. Development of the UV–visible spectra recorded from the aqueous phase during the polymerization of pyrrole. The detected oligomers correspond to the following samples: (a) PPy/NO_3, (b) PPy/DTAB, (c) PPy/SDS, and (d) PPy/Ag.

two bands develop at 471 (2.48 eV) and 510 nm (2.29 eV) for PPy/NO_3 and 436 (2.71 eV) and 461 nm (2.53 eV) for both PPy/SDS and PPy/DTAB. These represent the $\pi-\pi^*$ and bipolaron excitations, respectively [14,16]. The peaks without the presence of surfactant are red shifted indicating increased length of the oligomers [14]. All samples with surfactants have their absorption peaks shifted to lower wavelengths. A possible interpretation is that the surfactant templates result in growing oligomers with shorter conjugation length. In agreement with previous studies [17], monomers diffuse in the micelles resulting in a template mediated polymerization that we believe is the reason for the blue-shift of the UV–visible bands. Finally, we note the development of a broad absorption band starting at 600–700 nm for the PPy/NO_3 and PPy/DTAB derivatives that continues to extend to the near-IR region, indicating that the oligomers are in the doped state, as has been previously reported for water soluble polypyrrole [14]. The beginning of this broad absorption was not observed in the PPy/SDS sample, probably, from reduced doping compared to the other samples. When Ag(I) was used, at the start of reaction only a small shoulder appears at 425 nm. As the reaction proceeded one band developed at 463 nm, which later was split in to two peaks centered at 434 (2.71 eV) and 463 nm (2.53 eV).

The PPy/Ag, PPy/NO_3, PPy/DTAB and PPy/SDS materials were further characterized by infrared spectroscopy. The spectra, Fig. 2, exhibit all characteristic vibrations from oxidized polypyrrole [18]. Thus, the vibrations at 1544 and 1455 cm^{-1} (pyrrole ring), 1300 (in plane =C–H) and 1175 cm^{-1} (C–N stretching) mark the presence of oxidized doped polypyrrole. Moreover, the absorptions at 915 and 784 cm^{-1}, characteristic of the $(py_3)^+$ cation in $[(py_3)^+A^-]$ associations, are also present in all samples [18]. The peak at 1385 cm^{-1} is attributed to the NO_3^- balancing anion [19]. The intensity of this peak is stronger for the PPy/Ag, PPy/NO_3 and PPy/DTAB derivatives compared to PPy/SDS, implying a lower NO_3 percentage in the PPy/SDS sample due to the counterion role of SDS molecules. Furthermore, the PPy/SDS and PPy/DTAB members exhibit characteristic peaks of the aliphatic chains at 2921 and 2850 cm^{-1}. The presence of these aliphatic vibrations and the absence of a strong NO_3^- peak are strong indications for the incorporation of the surfactant in the polymer main chain.

The crystallinity and consequently the chain packing of the synthesized polymers were examined by X ray diffraction analysis. The respective XRD patterns, Fig. 3, unveil slight differences in the chain packing for the three derivatives. All the polypyrrole films exhibit mostly amorphous patterns with a broad scattering maximum centered at $2\theta = 24^\circ$, which has been previously observed in polypyrrole structures from different synthetic methods [20]. The band at 24° originates

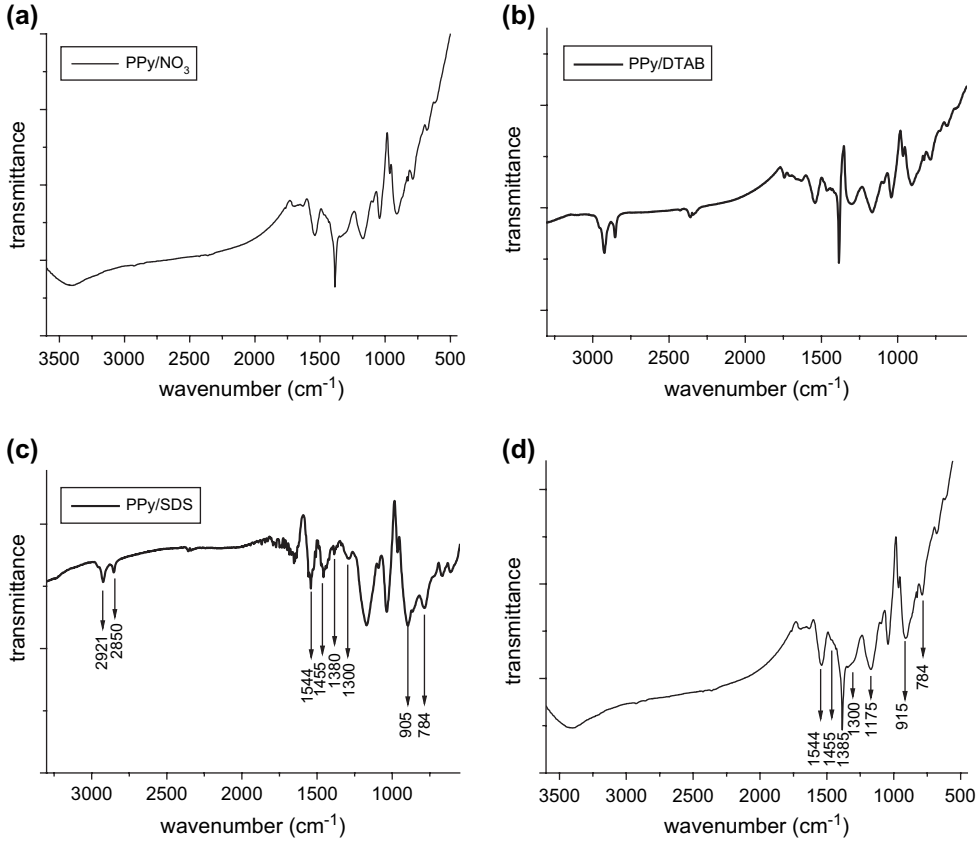

Fig. 2. Infrared spectra: (a) PPy/NO_3, (b) PPy/DTAB, (c) PPy/SDS, and (d) PPy/Ag.

from limited face to face stacking of pyrrole rings [21]. As the three patterns are almost identical we can assume that their structures are similar and imply a low crystallinity with large amorphous regions. The sharp reflections at 4°, 8.1°, 12°, 16.2° and 21° superimposed on the broad bands in the PPy/DTAB arise from a layered structure of DTAB ion pairs entrapped in the polymer matrix and possibly from an enhanced ordering of the macromolecular chains due to the template role of the surfactant.

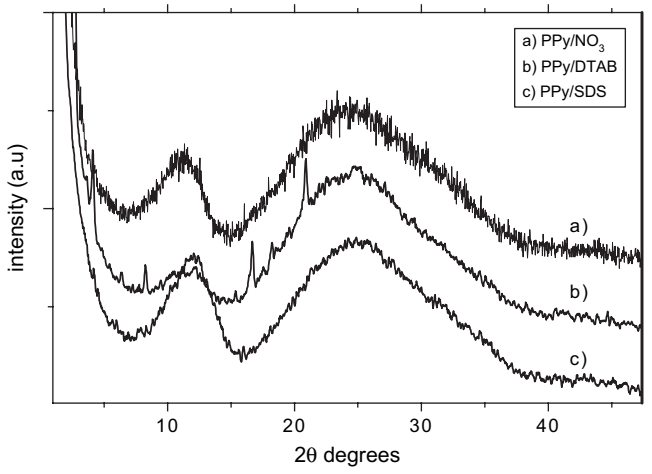

Fig. 3. XRD patterns of the following polypyrrole samples: (a) PPy/NO_3, (b) PPy/DTAB, and (c) PPy/SDS.

The XRD pattern of the nanocomposite indicated the crystal structure of the resulting polymer and the incorporation of the silver nanoparticles (Fig. 4). The polymer exhibits a similar with the other polypyrrole samples, amorphous pattern (in the range $2\theta = 1-35°$), providing a strong indication that the different oxidants do not affect the crystal structure of

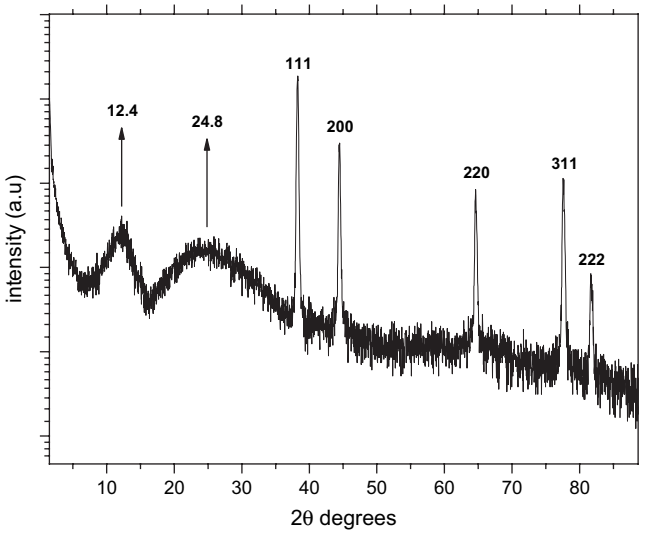

Fig. 4. XRD pattern of the silver/PPy nanocomposites. The broad diffractions at low 2θ degrees (1–35°) arise from the polymer chains and the sharp peaks from the Ag particles.

polypyrrole. At higher 2θ degrees the intense diffraction peaks due to silver nanoparticles are clearly seen at the following 2θ degrees with the corresponding crystal plains given in parentheses: 38.5° (111), 44.5° (200), 64.7° (220), 77.7° (311) and 81.5° (222) [22]. As expected due to the higher scattering intensity of the metal nanoparticles compared to the amorphous organic polypyrrole structures, the peaks assigned to the silver crystal plains appear with a higher intensity than the bands of polypyrrole.

The morphological characteristics of the polypyrrole samples were examined by scanning electron microscopy. The polymers exhibit a chain-like morphology consisting of blocks with a diameter ranging between 200 and 300 nm depending on the addition or not of surfactants. These blocks are mutually connected to form extensive networks with a length of several microns. An almost uniform size distribution of the blocks is obtained for all the samples, independent of the addition or not of surfactants. This finding demonstrates that the interface procedure results in a controllable polymerization reaction with homogenously dispersed nucleation centers.

Polypyrrole synthesized without surfactant (Fig. 5) exhibits a coral-like morphology with randomly directed parts. In contrast to the other two samples, this polymer structure does not present a symmetrical orientation, but it is grown randomly without exhibiting distinctive particles.

In the surfactant assisted polymerizations, the primary blocks are smaller, especially when sodium dodecylsulfate was used. In this case, some blocks are assembled in a linear constantly expanding chain-like network (Fig. 6). In previous works, concerning the oxidative polymerization of pyrrole in the presence of surfactants, various morphologies have been reported which are highly dependent on the surfactant used [23]. It is well known that anionic surfactants react electrostatically with the polymer polycations, while in general the hydrophobic part of the surfactant molecule may absorb on the polymer chain [23]. Thus, in order to explain the observed structures we propose that the surfactants spread on the water phase to form isolated monolayer films with the polar groups

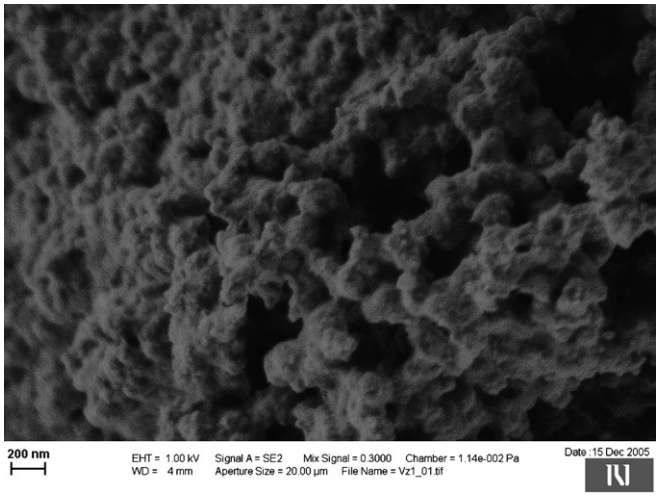

Fig. 6. Scanning electron microscopy image of the PPy/SDS sample.

headed to the aqueous and the aliphatic chains to the organic phase. Monomers diffuse preferentially to this templating area whereby encountering the incoming trivalent iron cations, the oxidative polymerization is carried out in a controllable way. In the case of SDS, as the polymerization proceeds, the dodecylsulfate anions act as counterbalance ions as alluded by the FT-IR spectroscopy, and force the monomer to grow in elongated geometries (Fig. 6).

In the case of DTAB the macromolecules grow in spheres that are bound together (Fig. 7). Previous work, referring to the use of this surfactant in the microemulsion polymerization of pyrrole, has demonstrated the templating role of spherical micelles that force the polymer to grow in spheres [17]. In a similar manner, we propose that templates of DTAB formed at the interface host the pyrrole monomer that polymerize upon penetration of the oxidizing Fe(III) cations. Since DTA^+ is positively charged, it cannot act as counterion and no elongated parts are observed. In all samples no tubular structures or linear fibers were observed demonstrating that the strong interchain interactions

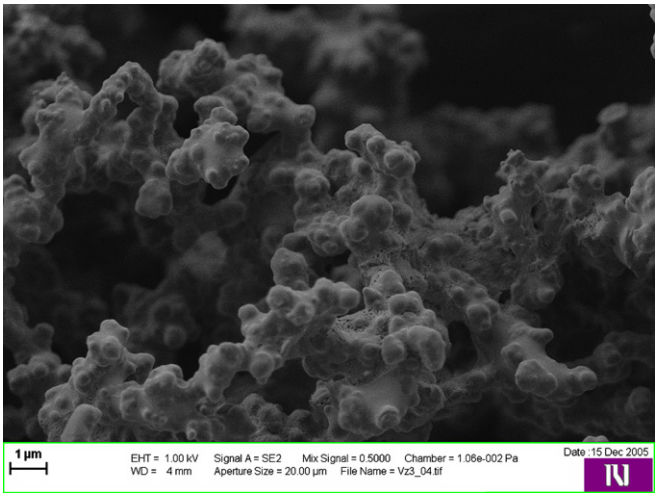

Fig. 5. Scanning electron microscopy image of the PPy/NO_3 sample.

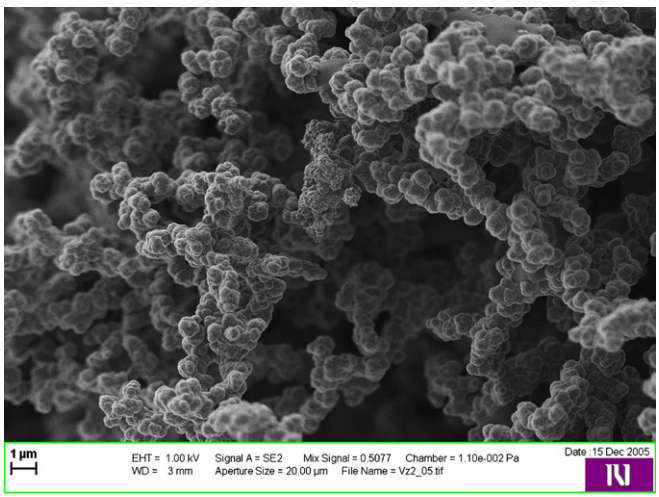

Fig. 7. Scanning electron microscopy image of the PPy/DTAB sample.

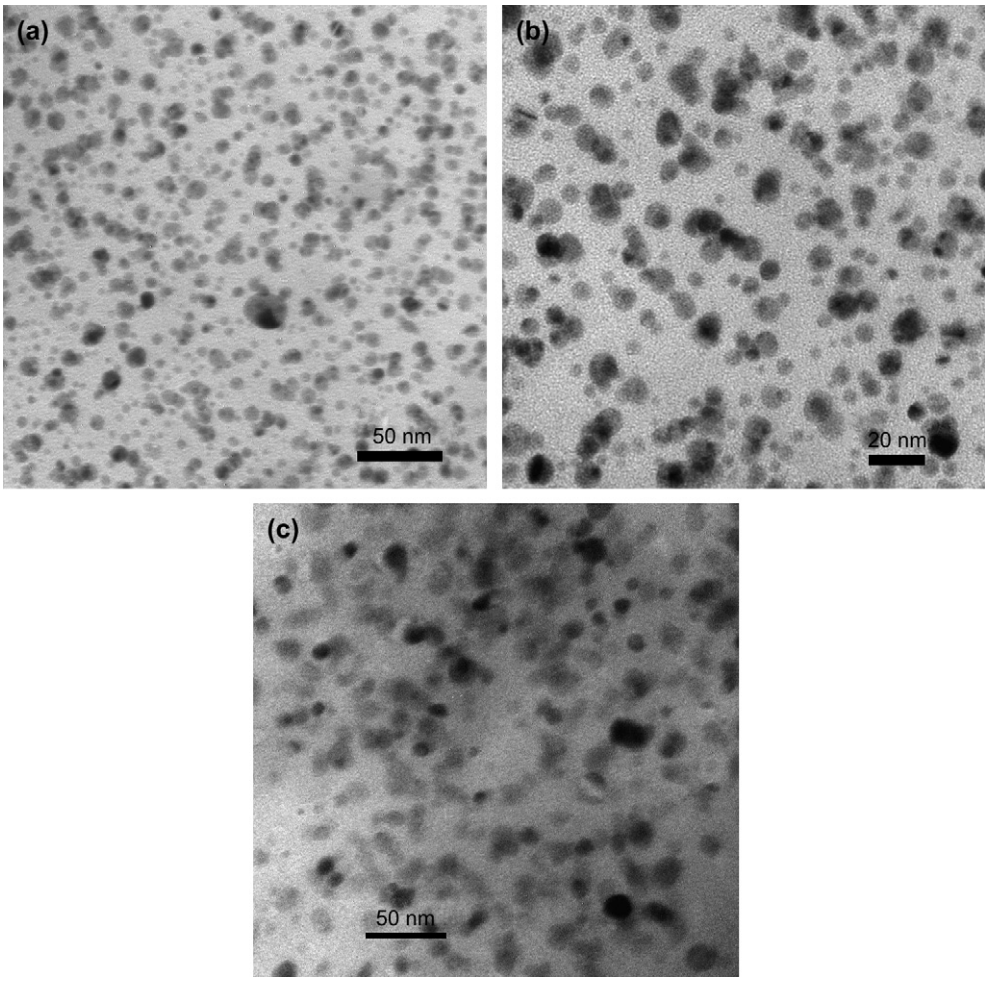

Fig. 8. TEM images in various scales showing the dispersion of spherical silver nanoparticles in the polypyrrole matrix.

of the polypyrrole macromolecules do not favor the formation of fibers or tubes without the use of hard templates.

Transmission electron microscopy micrographs of the thin film shown in Fig. 8 in conjunction with the corresponding X ray diffraction patterns indicate the formation of silver nanoparticles dispersed in the polypyrrole matrix. The interfacial polymerization yields spherical nanoparticles that although, are not clearly monodispersed, have a narrow size distribution. The narrow size distribution (mean diameter about 10 nm) and the homogenous dispersion result from the interfacial system and the absence of stirring during the polymerization. However, a low percent of larger particles with a diameter close to 30 nm and a limited agglomeration were also observed (Fig. 8c). The formation of the silver nanoparticles results from the oxidative action of the Ag^+ cations in the pyrrole polymerization. The nitrate ions (NO_3^-) from $AgNO_3$ are incorporated to the polypyrrole backbone where they act as counterions as shown by the FT-IR results. The simultaneous growth of polypyrrole chains alongside with the reduction of silver cations results first in the isolation of the nucleation centers and further to the growth of spherical nanoparticles that remain incorporated in the polypyrrole matrix. Summarizing the UV–visible and TEM data, it is concluded that even if a limited polymerization occurs in the aqueous phase as indicated by the UV–visible spectra, the entrapment of the silver nanoparticles in the pyrrole matrix is a strong indication that the reaction proceeds almost exclusively at the interface.

Finally, the thermal stability of the PPy polymers was studied by thermogravimetric analysis measurements under air flow. The TGA curves (Fig. 9) show a weight loss up to 120 °C which is due to evaporation of absorbed solvent, and from 150 to 250 °C due to the surfactant decomposition for the PPy/SDS and PPy/DTAB samples. The thermal stability of the synthesized polymers is lower compared to previous reports [23], probably, due to a lower molecular weight. For PPy/DTAB the weight loss between 200 and 250 °C is a strong indication that the surfactants participate in the growth of the polypyrrole spheres and are entrapped or physisorbed in the nanospheres. Polypyrrole samples with long alkyl chain surfactants exhibit a higher weight loss compared to PPy/NO_3. Furthermore, the weight percentage of silver in the PPy/Ag nanocomposite can be calculated from the thermogravimetric results and is about 65% of the total weight (Fig. 9d).

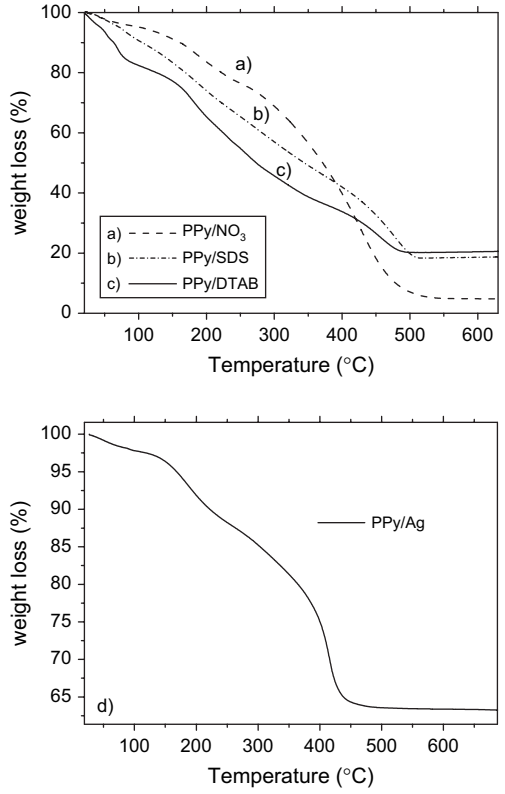

Fig. 9. TGA thermographs recorded under air flow for the following samples: (a) PPy/NO_3, (b) PPy/SDS, (c) PPy/DTAB, and (d) PPy/Ag.

5. Conclusions

We have described the interfacial polymerization of pyrrole which is also applied for the synthesis of silver/polypyrrole nanocomposites. The presence of the surfactant molecules in the polymer mass was established with FT-IR spectroscopy. The electron microscopy images unveil the different morphological characteristics of polypyrrole according to the addition or not of various surfactants as well as the size and shape of the silver nanoparticles. The main advantage of the interfacial polymerization is that it is a controllable and slow reaction in contrast with the conventional aqueous phase polymerization. Instead of silver, various other noble metal cations can be used leading to various polypyrrole nanocomposites.

References

[1] Aleshin AA. Adv Mater 2006;18:17–27.
[2] Wu CG, Bein T. Science 1994;264:1757.
[3] Martin CR. Chem Mater 1996;8:1739.
[4] Wang CW, Wang Z, Li MK, Li HL. Chem Phys Lett 2001;341:431.
[5] Qiu HJ, Wan MX. J Polym Sci A Polym Chem 2001;39:3485–97.
[6] Huang LM, Wang ZB, Wang HT, Cheng XL, Mitra A, Yan YX. J Mater Chem 2002;12:388.
[7] Liu JM, Yang SC. Chem Commun 1991;21:1529–30.
[8] Zhang L, Wan M. Nanotechnology 2002;13:750–5.
[9] (a) Zhang X, Manohar SK. J Am Chem Soc 2004;126:12714–5;
(b) Zhang X, Manohar SK. J Am Chem Soc 2005;127:14156.
[10] Yang Y, Chu Y, Yang F, Zhang Y. Mater Chem Phys 2005;92:164.
[11] Huang J, Virji Sh, Weiller BH, Kaner RB. J Am Chem Soc 2003;125:314–5.
[12] Atay T, Song JH, Nurmikko AV. Nano Lett 2004;4(9):1627–31.
[13] Xu G, Chen Y, Tazawa M, Jin P. J Phys Chem B 2006;110:2051–6.
[14] (a) Chen A, Kamata K, Nakagawa M, Iyoada T, Wang H, Li X. J Phys Chem B 2005;109:18283;
(b) Bae WJ, Kim KH, Jo HW. Macromolecules 2005;38:1044.
[15] Dallas P, Georgakilas V, Niarchos D, Komninou Ph, Kehagias G, Petridis D. Nanotechnology 2006;17:2046–53.
[16] Bredas JL, Scott JC, Yakushi K, Street B. Phys Rev B 1984;30(2):1023–5.
[17] Jang J, Li XL, Oh JH. Chem Commun 2004;794.
[18] (a) Oh EJ, Jang KS, MacDiarmid AG. Synth Met 2002;125:267;
(b) Ghosh S, Bowmaker GA, Cooney RP, Seakins JM. Synth Met 1998;95:63.
[19] Nakanishi Koji. Infrared absorption spectroscopy. San Francisco: Holden Day Inc; 1964.
[20] Buckley LJ, Roylance DK, When GE. J Polym Sci Polym Phys Ed 1987;25:2179.
[21] Wynne KJ, Street JB. Macromolecules 1985;18:2361.
[22] Parikh AN, Schivley MA, Koo E, Seshadri K, Aurentz DK, Mueller K, et al. J Am Chem Soc 1997;119:3135.
[23] Omastova M, Trchova M, Kovarova J, Stejskal J. Synth Met 2003;138:447.